

Computational study for investigating acoustic streaming and heating during acoustic hemostasis.

Maxim A. Solovchuk^{1*} Marc Thiriet² Tony W. H. Sheu^{1,3†}

¹ Center of Advanced Study in Theoretical Sciences (CASTS), National Taiwan University

² Sorbonne Universities, UPMC Univ Paris 06, UMR 7598, Laboratoire Jacques-Louis Lions, F-75005, Paris, France

³ Department of Engineering Science and Ocean Engineering, National Taiwan University,
No. 1, Sec. 4, Roosevelt Road, Taipei, Taiwan 10617, Republic of China

January 27, 2022

Abstract

High intensity focused ultrasound (HIFU) has many applications ranging from thermal ablation of cancer to hemostasis. Although focused ultrasound can seal a bleeding site, physical mechanisms of acoustic hemostasis are not fully understood yet. To understand better the interaction between different physical mechanisms involved in hemostasis a mathematical model of acoustic hemostasis is developed. This model comprises the nonlinear Westervelt equation and the bioheat equations in tissue and blood vessel. In the three dimensional domain, the nonlinear hemodynamic equations are coupled with the acoustic and thermal equations. Convected cooling and acoustic streaming effects are incorporated in the modeling study. Several sonication angles and two wound shapes have been studied. The optimal focal point location is at the rear of the wound and the optimal angle is 45° .

Keywords: *acoustic hemostasis; HIFU; Navier-Stokes equations; acoustic streaming; Westervelt equation*

1 Introduction

Bleeding is one of the major causes of death after traumatic injuries [1]. Management of this type of injuries in 1987 in the USA, for example, accounted for \$64.7 billion (in 1993 dollars) [2, 3]. Hemorrhage is stopped by vessel ligation, clamping, and repair of the vessel [4, 5].

Acoustic hemostasis is a new field of ultrasound research. Focused ultrasound has been successfully applied to the treatment of tumors in different areas of the bodies, including the breast, prostate, uterine fibroids and liver [6, 7]. Other promising applications of high intensity focused ultrasound (HIFU) include small blood vessel occlusion [8–10], hemostasis of bleeding vessels and organs [11–13] by delivering a large amount of acoustic energy to the bleeding site.

*solovchuk@gmail.com

†twhsheu@ntu.edu.tw.

Although numerous experimental studies have been performed, the optimal strategy for the acoustic hemostasis is not very clear. The ultrasound frequency, intensity, duration of treatment, location of focal point differ a lot in different experimental studies. The focus can be fixed at the center of the wound, its proximal or its distal part. Ultrasound focus can be also moved continuously along the wound. Multiple sonications at several points can be used as well. Several studies have been performed for punctured blood vessel [1, 12, 14]. Under the same ultrasound parameters, the treatment time can differ even by an order of magnitude for similar punctures [14]. The difference can be attributed to the wound shape and the guidance of HIFU. Ultrasound beam should be precisely located on the wound. If the location of the focal point was not strictly controlled, a very large increase in treatment time was required. In order to improve the treatment planning processes involved during acoustic hemostasis should be understood.

Most of the acoustic hemostasis studies have been performed experimentally. There were only a few numerical studies [15–17]. In Ref. [15] ultrasound propagation through different coupling materials between the tissue and transducer was studied. Heating in homogeneous media was considered. [17] studied the effects of blood flow cooling and acoustic streaming on ultrasound heating. Low intensity ultrasound with peak pressures up to 2 MPa was considered. They assumed a classical thermoviscous medium in which the absorption increases as frequency squared. For tissues the power law for absorption is more close to the linear dependence on frequency f^1 . For high ultrasound powers and large peak pressures used in acoustic hemostasis applications this assumption is not valid. In order to take into account the correct absorption law, relaxation effect should be taken into account [18]. Recently, a three dimensional model for the determination of the influences of blood flow and the acoustic streaming on the temperature distribution was presented [18, 19]. The proposed model was applied to get the temperature elevation in liver tumor in a patient specific geometry [20]. In the present paper the developed mathematical model will be applied to the acoustic hemostasis. Importance on the thermal and acoustic streaming effects will be addressed.

Numerous experimental studies [12, 14, 21] on acoustic hemostasis have provided strong evidence that the thermal effect of focused ultrasound is responsible for the hemostasis. The absorbed ultrasound energy in tissues is transformed into the thermal energy during focused therapy and this energy deposition can quickly cause the tissue temperature to increase. Temperature elevation in excess of 70°C in about 1 second [12] allows sealing of the bleeding site. Blood flow at the wound can in theory carry away part of the deposited energy making the temperature elevation at the wound more complicated. In the experiments [14] when the puncture site was exposed to the air, a jet of blood appeared out of the artery after the puncture. Such a jet flow can be stopped after focused ultrasound energy being applied to the bleeding site. In most of the experimental studies ultrasound beam was oriented perpendicularly to the wound. In the present paper several sonication angles and two wound shapes have been studied. We will show that sonication angle and focal point location can be optimized in order to decrease the amount of bleeding.

2 Methods

The three-dimensional (3D) acoustic-thermal- hydrodynamic coupling model has been proposed to compute the pressure, temperature, and blood flow velocity [18]. The mathematical model [18, 19] relies on a coupling of: (1) nonlinear Westervelt equation with relaxation effects being taken into account; (2) heat equations in biological tissues; and (3) acoustic streaming hydrodynamic equations.

2.1 Nonlinear acoustic equation

Acoustic field generated by a HIFU source was modeled using the coupled system of two partial differential equations given below [18]

$$\begin{aligned} \nabla^2 p - \frac{1}{c_0^2} \frac{\partial^2 p}{\partial t^2} + \frac{\delta}{c_0^4} \frac{\partial^3 p}{\partial t^3} + \frac{\beta}{\rho_0 c_0^4} \frac{\partial^2 p^2}{\partial t^2} + \sum_i P_i &= 0 \\ (1 + \tau_i \frac{\partial}{\partial t}) P_i &= \frac{2}{c_0^3} c_i \tau_i \frac{\partial^3 p}{\partial t^3} \end{aligned} \quad (1)$$

The above system of equations takes into account effects of diffraction, absorption, nonlinear propagation and relaxation effects. In the above, p is the sound pressure, $\beta = 1 + \frac{B}{2A}$ the coefficient of nonlinearity, and δ the diffusivity of sound originating from fluid viscosity and heat conduction, τ_i the relaxation time and c_i the small signal sound speed increment for the i -th relaxation process. The first two terms describe the contribution of linear lossless wave propagating at a small-signal sound speed. The third term denotes the loss resulting from thermal conduction and fluid viscosity. The fourth term accounts for acoustic nonlinearity which may considerably affect thermal and mechanical changes within the tissue. The last term models the inevitable relaxation processes. In the present paper two relaxation processes ($i = 2$) were considered. All the unknown relaxation parameters shown above were calculated through the minimization of a mean square error between the linear attenuation law and the relaxation model [18].

For the linear Westervelt equation the intensity is equal to $I_L = p^2/2\rho c_0$. For the nonlinear case the total intensity is

$$I = \sum_{n=1}^{\infty} I_n, \quad (2)$$

where I_n are the corresponding intensities for the respective harmonics nf_0 . The ultrasound power deposition per unit volume is calculated by

$$q = \sum_{n=1}^{\infty} 2\alpha(nf_0)I_n \quad (3)$$

The absorption coefficient in tissue shown above obeys the following frequency law:

$$\alpha = \alpha_0 \left(\frac{f}{f_0} \right)^\eta, \quad (4)$$

where $\alpha_0 = 8.1 \text{ Np/m}$, $\eta = 1.0$ and $f_0 = 1 \text{ MHz}$ [23].

2.2 Energy equation for tissue heating

In the current simulation study of thermal field the physical domain has been split into the domains for the perfused tissue and the flowing blood. In a region free of large blood vessels, the diffusion-type Pennes bioheat equation [24] given below is employed to model the transfer of heat in the perfused tissue region

$$\rho_t c_t \frac{\partial T}{\partial t} = k_t \nabla^2 T - w_b c_b (T - T_\infty) + q \quad (5)$$

In the above bioheat equation proposed for the modeling of time-varying temperature in the tissue domain, ρ , c , k denote the density, specific heat, and thermal conductivity, respectively. The subscripts t and b refer to the tissue and blood domains. The notation T_∞ is denoted as the temperature at a remote location. The variable w_b ($\equiv 0.5 \text{ kg/m}^3\text{-s}$) in Eq. (5) is the perfusion rate for the tissue cooling in capillary flows.

In the region containing large vessels, within which the blood flow can convect heat, the biologically relevant heat source, which is q , and the heat sink, which is $-\rho_b c_b \underline{\mathbf{u}} \cdot \nabla T$, are added to the conventional diffusion-type heat equation

$$\rho_b c_b \frac{\partial T}{\partial t} = k_b \nabla^2 T - \rho_b c_b \underline{\mathbf{u}} \cdot \nabla T + q \quad (6)$$

In the above, $\underline{\mathbf{u}}$ is the blood flow velocity. We note here that the above thermal equations (5,6) are coupled with the acoustic equations (1) for the acoustic pressure through the power deposition term q defined in Eq. (3).

2.3 Acoustic streaming hydrodynamic equations

Owing to the inclusion of heat sink shown on the right hand side of Eq. (6), the blood flow velocity plus the velocity generated from the acoustic streaming due to the applied high-intensity ultrasound must be determined. In this study the flow in large blood vessels is assumed to be incompressible and laminar. The vector equation for modeling the blood flow motion, subject to the divergence free equation $\nabla \cdot \underline{\mathbf{u}} = 0$, in the presence of acoustic stress vector is as follows [22, 25]

$$\frac{\partial \underline{\mathbf{u}}}{\partial t} + (\underline{\mathbf{u}} \cdot \nabla) \underline{\mathbf{u}} = \frac{\mu}{\rho} \nabla^2 \underline{\mathbf{u}} - \frac{1}{\rho} \nabla \mathbf{P} + \frac{1}{\rho} \underline{\mathbf{F}} \quad (7)$$

In the above, \mathbf{P} is the static pressure, μ ($= 0.0035 \text{ kg/m s}$) the shear viscosity of blood flow, and ρ the blood density. In Eq. (7), the force vector $\underline{\mathbf{F}}$ acting on blood fluid due to an incident ultrasound is assumed to act along the acoustic axis $\underline{\mathbf{n}}$ and has the following form [26, Ch. 7]

$$\underline{\mathbf{F}} \cdot \underline{\mathbf{n}} = -\frac{1}{c_0} \nabla \vec{I} = \frac{q}{c_0} \quad (8)$$

2.4 Solution procedure and description of the problem

Nonlinear Westervelt equation (1) is solved by finite difference method presented in Ref. [18]. Discretization of this system of differential equations is started with the approximation of the temporal

derivative $\frac{\partial}{\partial t} P_i^{n+1}$ shown in the second equation of the system (1):

$$\frac{\partial}{\partial t} P_i^{n+1} = \frac{1}{2\Delta t} (3P_i^{n+1} - 4P_i^n + P_i^{n-1}) \quad (9)$$

After some algebraic manipulation the second equation in the system (1) can be rewritten in the form:

$$P_i^{n+1} = \frac{2}{c_0^3} \frac{c_i \tau_i}{1 + 1.5\tau_i/\Delta t} \frac{\partial^3 p^{n+1}}{\partial t^3} - \frac{\tau_i}{2\Delta t + 3\tau_i} (-4P_i^n + P_i^{n-1}) \quad (10)$$

P_v^{n+1} is then substituted into the first equation of the system (1). The resulting equation will be solved implicitly.

Temporal derivatives in Westervelt equation are approximated using the following second order accurate schemes:

$$\left. \frac{\partial^2 p}{\partial t^2} \right|^{n+1} = \frac{2p^{n+1} - 5p^n + 4p^{n-1} - p^{n-2}}{(\Delta t)^2} \quad (11)$$

$$\left. \frac{\partial^3 p}{\partial t^3} \right|^{n+1} = \frac{6p^{n+1} - 23p^n + 34p^{n-1} - 24p^{n-2} + 8p^{n-3} - p^{n-4}}{2(\Delta t)^3} \quad (12)$$

The nonlinear term $\left. \frac{\partial^2 p^2}{\partial t^2} \right|^{n+1}$ is linearized using the second order accurate relation:

$$\begin{aligned} \left. \frac{\partial^2 p^2}{\partial t^2} \right|^{n+1} &= \frac{\partial}{\partial t} \left(\left. \frac{\partial p^2}{\partial t} \right|^{n+1} \right) = 2 \frac{\partial}{\partial t} \left(p^n \left. \frac{\partial p}{\partial t} \right|^{n+1} + p^{n+1} \left. \frac{\partial p}{\partial t} \right|^n - p^n \left. \frac{\partial p}{\partial t} \right|^n \right) = \\ &= 2 \left(2p_t^n p_t^{n+1} + p^n p_{tt}^{n+1} + p^{n+1} p_{tt}^n - (p_t^n)^2 - p^n p_{tt}^n \right) \end{aligned} \quad (13)$$

The above equations are then substituted into the Westervelt equation to get the Helmholtz equation. This equation is then solved using the three-point sixth-order accurate scheme [18]. Accuracy of the numerical solutions was examined in [18] by comparing them with the known analytical and numerical solutions obtained by other authors [27, 28]. Good agreement between the measured and numerical results was also obtained [18, 19].

First the acoustic pressure was calculated. The acoustic pressure was calculated only once for a given set of transducer parameters. Afterwards, ultrasound power deposition in Eq. (3) and acoustic streaming force in Eq. (8) were determined and stored. Blood flow velocity was computed from Eq. (7) at every time step with the acoustic streaming effect being taken into account and then was substituted to the bioheat equation (6). With the known blood flow velocities and power deposition terms, temperatures in blood flow domain and in tissue were calculated. Initially, temperature is considered to be equal to 37°C. Temperature continuity at the fluid-solid interface is imposed as that being applied in a conjugate heat transfer problem. The interface boundary condition takes into account the thermal conduction in tissue and convection in blood vessel domain. The three-dimensional problem is analyzed using finite-volume method. A detailed description of the solution procedures can be found in our previous articles [18, 19, 25].

The present 3D computational model was validated by comparing our simulated results for the temperature field, with and without flow, with the experimental results of Huang et al. [17]. The computational model for the prediction of acoustic streaming field was validated by comparing the results

with those of Kamakura et al. [22]. Temperature elevation by HIFU in ex-vivo porcine muscle was studied experimentally as well by MRI and numerically [29]. We demonstrated that for peak temperatures below 85-90°C our numerical simulation results are in excellent agreement with the experimental data measured in three dimensions. Both temperature rise and lesion size can be well predicted. For peak temperatures above 85-90°C preboiling or cavitation activity appears and, by consequence, lesion distortion starts, causing a small discrepancy between the measured and simulated temperature rises.

In the present paper the vessel with a diameter of 3 mm is considered. The fully developed velocity profile is prescribed at the inlet of blood vessel, while zero gradient velocity boundary condition is applied on the outlet plane. The pressure at the wound is equal to the tissue pressure. At vessel inlet, the blood flow cross-sectional average velocities are set at 0.016 m/s and 0.13 m/s. These imposed velocities correspond to the velocities in veins and arteries with the diameter of 3 mm [30]. Two wound shapes, namely, the small circular wound with a diameter of 2 mm and a big wound of 6 mm in length and 2 mm in diameter will be investigated (Fig. 1).

The single element HIFU transducer used in this study is spherically focused with an aperture of 12 cm and a focal length of 12 cm. In this study, the transducer with the frequency $f_0 = 1.0$ MHz is considered. Focal intensity is 2240 W/cm², and the sonication time is 0.6 second. The parameters used in the current simulation are listed in Table 1 [23].

Table 1: Acoustic and thermal properties for the tissue and blood.

Tissue	c_0 ($\frac{m}{s}$)	ρ ($\frac{kg}{m^3}$)	c ($\frac{J}{kgK}$)	k ($\frac{W}{mK}$)	α ($\frac{Np}{m}$)
tissue	1540	1055	3600	0.512	8.1f
Blood	1540	1060	3770	0.53	1.5f

3 Results and discussion

As it was already mentioned in introduction, heating is considered as one of the main consequences during acoustic hemostasis. Increase of the temperature above a certain value allows cauterizing of the bleeding site. The temperature of 70°C can be assumed as the threshold temperature for the acoustic hemostasis [12]. However, blood flow out of the wound may carry away the heat at the bleeding site and significantly reduce the temperature at the bleeding site. Blood also has a lower absorption than a tissue. For example, in Table 1 it can be seen that absorption coefficients of liver tissue and blood differ by about five times. Therefore if blood is still flowing out of the wound it is quite difficult to seal the wound. First of all, it is necessary to reduce or stop the flow out of the wound, then thermal energy can be applied to cauterize the bleeding site and seal the wound. In the experiments [14] with the wound exposed to air it was shown that blood flow out of the wound can be stopped after applying focused ultrasound energy to the bleeding site. Focused ultrasound induces streaming of the blood away from the focus of the transducer. This effect is called acoustic streaming. Thus, physical processes involved

in acoustic hemostasis can be described in the following way: first, acoustic streaming effect reduces or stops the flow out of the wound, afterwards thermal effect is used to seal the wound. In the following sections we are going to investigate numerically the acoustic streaming effect for two wound shapes and different sonication angles and thermal effect for different sonication angles.

3.1 Importance of acoustic streaming

3.1.1 Bleeding in a small wound

In the previous studies [18, 19] it was shown that focused ultrasound can induce acoustic streaming velocities up to 100 cm/s in the blood vessel and can affect the ultrasound heating. When blood vessel was placed perpendicularly to the acoustic axis, acoustic streaming velocity magnitude becomes smaller comparing with that of the parallel blood vessel orientation.

When the focus of HIFU transducer is directed towards a bleeding site, the local absorption of acoustic energy supplies an extra momentum to the fluid and this force can result in streaming of the blood in the direction away from the focus of transducer. Usually in the acoustic hemostasis experiments blood vessel was located perpendicularly to the acoustic axis. However it is not very clear what blood vessel orientation is the optimal one. For the case of big wound different focal point locations and scanning path planning can be chosen differently. So we are going to investigate the effects of blood vessel orientation (sonication angle) and focal point location.

Let's consider a hole (wound) on the blood vessel wall. The diameter of this hole is 2 mm. The diameter of the blood vessel is 3 mm, and the maximum velocities are 3.2 cm/s (vein) and 26 cm/s (artery). Acoustic streaming velocity magnitude is 30 cm/s (without acoustic streaming the maximum velocity in the vein is 3 cm/s). Acoustic streaming velocity magnitude is one order of magnitude larger than the blood flow velocity in the vein.

In Figs. 2, 3 the velocity profiles in vein and artery are presented with and without incident focused ultrasound. In Tables 2, 3 mass fluxes at the inlet and two outlets (outlet and wound) are presented in the vein and in the artery. Mass flux at the vessel inlet is equal to 100%. Without AS, 78% of the total mass flux comes out of the wound. If we switch the transducer, radiation force will cause the acoustic streaming flow to occur. With the acoustic streaming effect being taken into account, the bleeding in the vein can be completely stopped. However, there is still a small bleeding out of the artery. In the artery the blood flow out of the wound can be reduced by an amount from 45 % to 29 %. In order to stop blood flow out of the wound, higher power depositions should be considered.

Simulations show that acoustic streaming velocity profile reaches the steady state within a very short time interval of 0.12 s, within which the bleeding can be stopped or sufficiently reduced. This prediction is in agreement with the experimental observations [14].

In the next section we will show that for different sonication angles blood flow can be stopped even in the artery.

3.1.2 Bleeding in a big wound

In Tables 4, 5 mass fluxes at the inlet and two outlets of the blood vessel with a big wound are presented for the cases with and without considering acoustic streaming effect. The focal point is located at the center of the wound. For a larger wound it is more difficult to stop bleeding. When we take into account the acoustic streaming effect the bleeding out of the wound in the vein can be stopped. However, there is still a flow of the blood out of the wound in the artery. The blood flow out of the wound in the artery is reduced from 74 % to 53 % of the total mass flux due to the acoustic streaming effect. In Fig. 4 velocity profiles in the artery are presented for the cases with and without focused ultrasound. It can be seen that the bleeding is stopped in the small focal area. This means that in the focal area we can seal the bleeding site by heating.

In Fig. 5 mass flux out of the wound is presented as the function of focal point location along the axis of the big wound. When the focal point is located at the rear of the wound, the largest mass flux and consequently the largest bleeding occur. When the focal point is located close to the front of the wound ($x = 0.0175$), the mass flux is minimal. Therefore to reduce the bleeding in the large wound, focal point should be located at the front of the wound. In Fig. 6 mass flux out of the wound as the function of time is presented at different focal point locations. Within 0.12 s blood flow becomes steady. The smallest mass flux occurs at the condition when the focal point is located at the front of the wound. The worst case happens when the focal point is located at the rear of the wound.

Several ways of ultrasound sonications can be applied to stop bleeding in the wound. In the work of [11] mechanical scanning of HIFU probe was used to stop bleeding in a punctured artery. The frequency of the scanning was 15 or 25 Hz, the amplitude of the scanning was equal to the length of the wound (5-10 mm). In Fig. 7 the predicted evolution of mass flux for the big wound is presented for the case of mechanical scanning of HIFU beam along the wound. Focal point was oscillating around the center of the wound with the frequency 25 Hz. We can see that mass flux value is oscillating around the value of mass flux for the central location of the focal point. Decrease of the oscillating frequency will lead to

Table 2: Acoustic streaming effect on the mass flux in the small wound in the vein ($u = 1.6$ cm/s).

Mass flux	Outlet	Wound	Inlet
Without AS	22 %	78 %	100 %
With AS	100 %	0	100 %

Table 3: Acoustic streaming effect on the mass flux in the small wound in the artery ($u = 13$ cm/s).

Mass flux	Outlet	Wound	Inlet
Without AS	55 %	45 %	100 %
With AS	71 %	29 %	100 %

the increased oscillating amplitude. The mass flux is very close to that of the case when the focal point is at the center of the wound.

Table 4: The effect of acoustic streaming on the mass flux in the big wound in the vein ($u = 1.6$ cm/s).

Mass flux	Outlet	Wound	Inlet
Without AS	3 %	97 %	100 %
With AS	100 %	0	100 %

Table 5: The effect of acoustic streaming on the mass flux in the big wound in the artery ($u = 13$ cm/s).

Mass flux	Outlet	Wound	Inlet
Without AS	26 %	74 %	100 %
With AS	47 %	53 %	100 %

3.1.3 Bleeding in a big wound. Different sonication angles.

In Fig. 8 the evolution of the predicted mass flow out of the big wound is presented for different sonication angles in the artery. Focal point is located at the center of the wound. The best sonication angles are from 0° to 90° . At the angle 0° it's possible to completely stop bleeding within 0.1 s. Because ultrasound beam is quite narrow, for 0° sonication it's quite difficult to locate the ultrasound beam precisely on the wound. For the sonication angle 45° there is only small bleeding at the rear of the wound (Fig. 9). In the experiments, 90° sonications were mostly used. From the simulation point of view, it is better to use 45° . The predicted velocity magnitude in the artery with the big wound for two different sonication angles 45° and 135° are presented in Fig. 9. For 135° sonication there is a reverse flow near the center of the wound. This reverse flow acts like a dam and therefore velocity magnitude in the beginning of the wound is increased. Comparison of the mass fluxes with and without AS for this sonication angle shows that 135° sonication increases bleeding and should be avoided in the treatment.

In Fig. 10 the evolution of the predicted mass flow out of the big wound is presented for the two sonication angles 45° and 135° and two locations of the focal point: at a location in front of the wound and at the rear of the wound. The corresponding velocity magnitude for the sonication angle 45° can be seen in Fig. 11. When the focal point is located at the rear of the wound and the angle is 45° , the bleeding can be stopped. When the focal point is located in front of the wound and the angle is 45° , there is still a small blood flow out of the wound at the rear of the wound. For 135° an opposite result is obtained. For 90° and 135° sonications focal point should be located at the front of the wound. The numerical simulations show that 135° sonication should be avoided, because in this case the degree of bleeding increases. The smallest mass flux occurs at 45° sonication when the focal point is located at

the rear of the wound. Sonication angles between 45 and 90 degrees should be considered in order to reduce the flow out of the wound. In some cases flow out of the wound can be stopped.

Although in the experiments 90° sonications are mostly used [14], we have shown that for a big wound the optimal focal point location is at the rear of the wound and the optimal angle is 45° . In this case the flow out of the wound can be completely stopped. However the wound is not sealed yet, we should apply thermal energy in order to cauterize the bleeding site. In the following section we are going to investigate the thermal effect of ultrasound for different sonication angles.

3.2 Thermal effects

Let's study the temperature distribution in the tissue and in the blood domain during acoustic hemostasis. In most of the experimental studies ultrasound beam was located perpendicularly to the blood vessel. However, the optimal angle between the blood vessel and ultrasound beam is not very clear and it is not always possible to locate ultrasound beam perpendicular to the blood vessel. We are going to investigate how different sonication angles affect the temperature elevation. We assumed that acoustic streaming effect has already stopped the flow out of the wound and the blood vessel is intact. Focal point is located on the blood vessel wall. Blood flow velocity in the vein is 1.6 cm/s. In Fig. 12 the predicted temperature contours at $t = 0.6$ s at the cutting plane $y = 0$ are presented for three different sonication angles. We can see a very small temperature increase inside the blood vessel.

The predicted acoustic streaming velocity at the cutting plane in the blood vessel without an externally applied flow is presented in Fig. 13 for three different sonication angles. The acoustic streaming velocity magnitudes are 34 cm/s, 36 cm/s and 60 cm/s for the sonication angles 90° , 45° (or 135°) and 0° (or 180°), respectively. The acoustic streaming velocity has the smallest value for 90° sonication and the largest value for 0° sonication. For all sonication angles, acoustic streaming velocity magnitude is up to an order of magnitude larger than velocity in blood vessel (1.6 cm/s in vein and 13 cm/s in artery). Therefore cooling due to acoustic streaming effect can prevail over the blood flow cooling and can represent the main cooling mechanism.

In Fig. 14 the predicted temperature is presented at the focal point as the function of time for different sonication angles. It can be seen that for 90° sonication the predicted temperature has the largest value and for 0° sonication the predicted temperature has the smallest value. For 45° and 135° sonications the predicted temperatures are almost the same (about 1°C difference), because acoustic streaming velocity magnitude (35 cm/s) is an order of magnitude larger than the velocity in blood vessel (1.6 cm/s) and acoustic streaming is the main cooling mechanism in this case. The temperature around 70°C on the blood vessel wall can be reached at $t = 0.6$ s for 90° sonication, for other sonication angles it will take a longer time to reach the temperature 70°C . This shows the possibility to stop bleeding theoretically. For a smaller blood vessel the effects of blood flow cooling and acoustic streaming will be smaller.

In the current subsection we assumed that there is no blood flow coming out of the wound. In this case the temperature around 70°C can be achieved quite rapidly ($t < 1$ s) and the wound can be sealed in a short time. Simulation shows that 90° sonication should be chosen in order to optimize the treatment.

Conclusions

The mathematical model for the simulation of acoustic hemostasis is proposed in the current paper. Our analysis is based on the nonlinear Westervelt equation with the relaxation effect being taken into account and the bioheat equations are applied in blood vessel and tissue domains. The nonlinear hemodynamic equation is also considered with the acoustic streaming effect being taken into account.

Both thermal and acoustic streaming effects have been investigated in the current paper. The importance of acoustic streaming was examined for different blood vessel orientations and focal point locations. Acoustic streaming velocity magnitude is up to 60 cm/s and this magnitude is several times larger than the velocity in blood vessel. If focused ultrasound beam is applied directly to the bleeding site, the flow out of a wound is considerably reduced due to acoustic streaming. Bleeding can be even completely stopped depending on the blood vessel orientation and the focal point location. As a result, the wound can be quickly sealed. Simulations show that the temperature around 70 °C can be achieved within a second on the blood vessel wall, if there is no flow out of the wound. The temperature inside blood vessel remains almost unchanged. Sonication angles between 45 and 90 degrees should be considered in order to reduce blood flow out of the wound. This simulation confirms the theoretical possibility of sealing the bleeding site by means of focused ultrasound. The blood vessel remains patent after the treatment.

Acknowledgement

The authors would like to acknowledge the financial support from the Center for Advanced Study in Theoretical Sciences and from the National Science Council of Republic of China under Contract No. NSC102-2811-M-002-125.

References

- [1] V. Zderic, A. Keshavarzi, M.L. Noble, M. Paun, S.R. Sharar, L.A. Crum, R.W. Martin, S. Vaezy, Hemorrhage control in arteries using high-intensity focused ultrasound: A survival study, *Ultrasonics*, 2006;44:46–53.
- [2] S. Vaezy, V. Zderic, Hemorrhage control using high intensity focused ultrasound, *International Journal of Hyperthermia*, 2007;23:203 – 211.
- [3] T.R. Miller, D.C. Lestina, Patterns in US medical expenditures and utilization for injury, 1987. *Am J Public Health* 1996;86:89-93.
- [4] O. M. Austin, H. P. Redmond, P. E. Burke, P. A. Grace and H. B. Bouchier, Vascular trauma - a review, *J. Am. Coll. Surg.*, 1995;28:59–70.
- [5] M. O. Perry, Vascular Trauma, *Adv. Surgery*, 1995;28:59–70.
- [6] Y. F. Zhou, High intensity focused ultrasound in clinical tumor ablation, *World J. Clin. Oncol*, 2011;2:8–27.
- [7] T. A. Leslie and J. E. Kennedy, High intensity focused ultrasound in the treatment of abdominal and gynaecological diseases, *Int. J. Hyperthermia*, 2007;23:173–182.
- [8] K. Hynynen, V. Colucci, A. Chung, F. Jolesz, Noninvasive arterial occlusion using MRI-guided focused ultrasound, *Ultrasound in Medicine and Biology*, 1996;22:1071–1077.
- [9] J. Serrone, H. Kocaeli, T. Douglas Mast, M.T. Burgess, M. Zuccarello, The potential applications of high-intensity focused ultrasound (HIFU) in vascular neurosurgery, *Journal of Clinical Neuroscience*, 2012;19:214–221.
- [10] P.W. Henderson, G.K. Lewis, N. Shaikh, A. Sohn, A.L. Weinstein, W.L. Olbricht, J.A. Spector, A portable high-intensity focused ultrasound device for noninvasive venous ablation, *Journal of Vascular Surgery*, 2010;51:707–711.
- [11] S. Vaezy, R. Martin, P. Kaczkowski, G. Keilman, B. Goldman, H. Yaziji, S. Carter, M. Caps, L. Crum, Use of high-intensity focused ultrasound to control bleeding, *Journal of Vascular Surgery*, 1999;29:533–542.
- [12] S. Vaezy, R. Martin, L. Crum, High intensity focused ultrasound: A method of hemostasis, *Echocardiography*, 2001;18:309–315.
- [13] S. Vaezy, R.W. Martin, U. Schmiedl, M. Caps, S. Taylor, K. Beach, S. Carter, P. Kaczkowski, G. Keilman, S. Helton, W. Chandler, P. Mourad, M., Rice, R., Roy, L., Crum, Liver hemostasis using high-intensity focused ultrasound, *Ultrasound in Medicine and Biology*, 1997;23:1413–1420.
- [14] S. Vaezy, R. Martin, H. Yazij, P. Kaczkowski, G. Keilman, S. Carter, M. Caps, E. Y. Chi, M. Bailey, L. Crum, Hemostasis of punctured blood vessels using high-intensity focused ultrasound, *Ultrasound Med Biol.*, 1998;24:903–910.

- [15] J.L. Teja, S.A. Lopez-Haro, L. Leija, A. Vera, A finite element simulation of High Intensity Focused Ultrasound with polyacrylamide as coupling material for acoustic hemostasis In proceeding of: Health Care Exchanges (PAHCE), 2013 Pan American.
- [16] X. Zeng, S. Mitchell, M. Miller, S. Barnes, J. Hopple, J. Kook, R. Moreau-Gobard, S. Hsu, A. Ahiekpor-Dravi, L. A. Crum, J. Eaton., K. Wong and K. M. Sekins, Acoustic hemostasis of porcine superficial femoral artery: Simulation and in-vivo experimental studies AIP Conference Proceedings, 2012;1481:475–480.
- [17] J. Huang, R. G. Holt, R. O. Cleveland, R. A. Roy, Experimental validation of a tractable medical model for focused ultrasound heating in flow-through tissue phantoms, J. Acoust. Soc. Am., 2004;116:2451–2458.
- [18] M. A. Solovchuk, T. W. H. Sheu, M. Thiriet, Simulation of nonlinear Westervelt equation for the investigation of acoustic streaming and nonlinear propagation effects, J. Acoust. Soc. Am., 2013;134:3931–3942.
- [19] M. A. Solovchuk, T. W. H. Sheu, M. Thiriet, W. L. Lin, "On a computational study for investigating acoustic streaming and heating during focused ultrasound ablation of liver tumor", J. of Applied Thermal Engineering, 2013;56:62-76.
- [20] M. A. Solovchuk, T. W. H. Sheu, M. Thiriet, "Image-based computational model for focused ultrasound ablation of liver tumor," Journal of Computational Surgery 1:4 (2014).
- [21] S. Vaezy, M.L. Noble, A. Keshavarzi, M. Paun, A.F. Prokop, C. Cornejo, S. Sharar, E.Y. Chi, L.A. Crum, R.W. Martin, Liver Hemostasis with High-Intensity Ultrasound: Repair and Healing, Journal of Ultrasound in Medicine, 2004;23:217–225.
- [22] T. Kamakura, M. Matsuda, Y. Kumamoto, M. A. Breazeale, Acoustic streaming induced in focused Gaussian beams, J. Acoust. Soc. Am., 1995;97:2740–2746.
- [23] F. A. Duck, Physical Property of Tissues - A comprehensive reference book, Academic, London, 1990.
- [24] H. H. Pennes, Analysis of tissue and arterial blood temperature in the resting human forearm, J. Appl. Physiol., 1948;1:93-122.
- [25] M. A. Solovchuk, T. W. H. Sheu, W. L. Lin, I. Kuo, and M. Thiriet, "Simulation study on acoustic streaming and convective cooling in blood vessels during a high-intensity focused ultrasound thermal ablation," Int. J. Heat and Mass Transfer, 2012;55:1261–1270.
- [26] M. F. Hamilton, D. T. Blackstock, Nonlinear Acoustics, Academic Press, Boston, 1998.
- [27] H. T. O'Neil, Theory of focusing radiators, J. Acoust. Soc. Am., 1949;21:516-526.
- [28] D. T. Blackstock, "Connection between the Fay and Fubini solutions for plane sound waves of finite amplitude," J. Acoust. Soc. Am., 1966;14:1019–1026.

- [29] M. A. Solovchuk, S. C. Hwang, H. Chang, M. Thiriet, T.W.H. Sheu, Temperature elevation by HIFU in ex-vivo porcine muscle: MRI measurement and simulation study. *Medical Physics* 2014; 41: 052903. <http://dx.doi.org/10.1118/1.4870965>
- [30] J. W. Hand, Ultrasound hyperthermia and the prediction of heating, in: F. A. Duck, A. C. Baker, H. C. Starritt (Eds.), *Ultrasound in Medicine* , Institute of Physics Publishing, Bristol, 1998, Ch. 8.

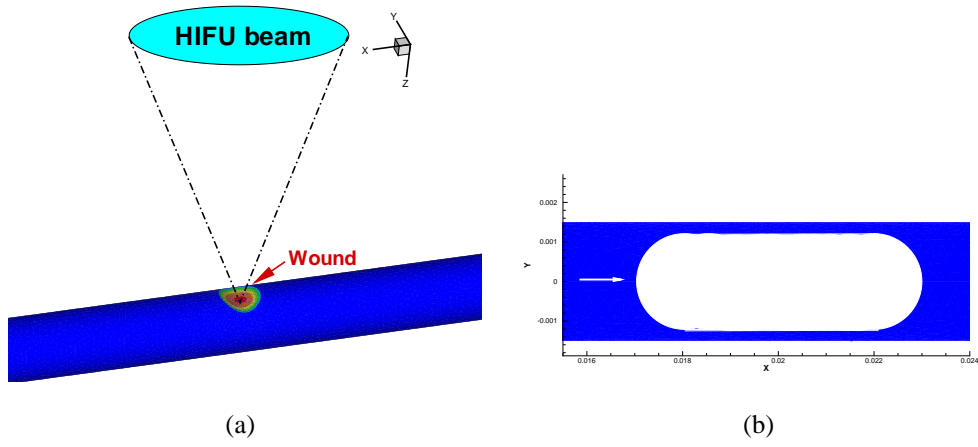


Fig. 1: Schematic of the problem. (a) a small wound with the diameter $d = 2$ mm in the blood vessel ($d = 3$ mm); (b) a big wound with the length 6 mm and the diameter 2 mm. The blood vessel diameter is 3 mm.

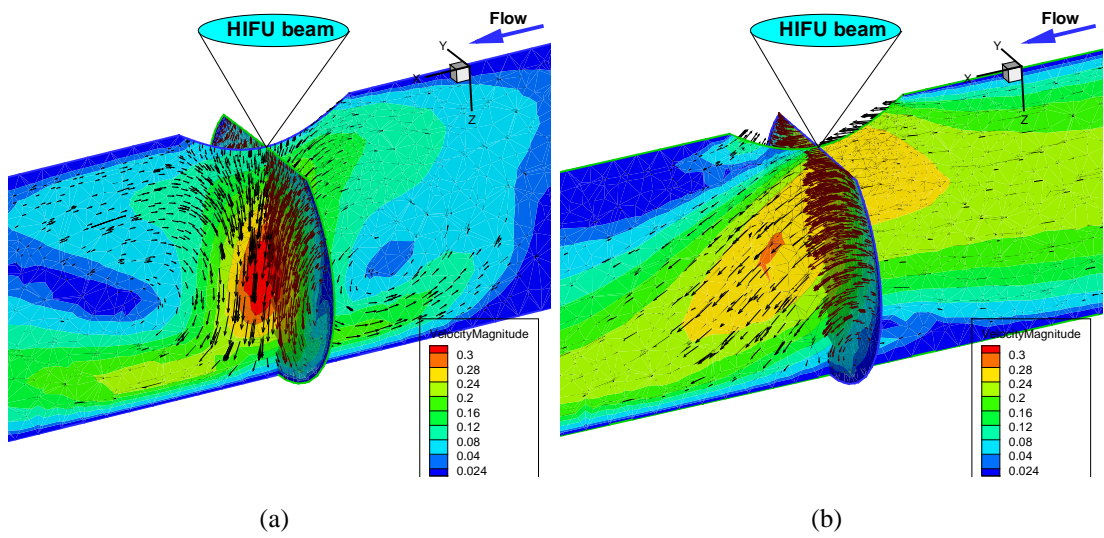


Fig. 2: The predicted velocity in vein (a) and artery (b) when the acoustic streaming effect is taken into account.

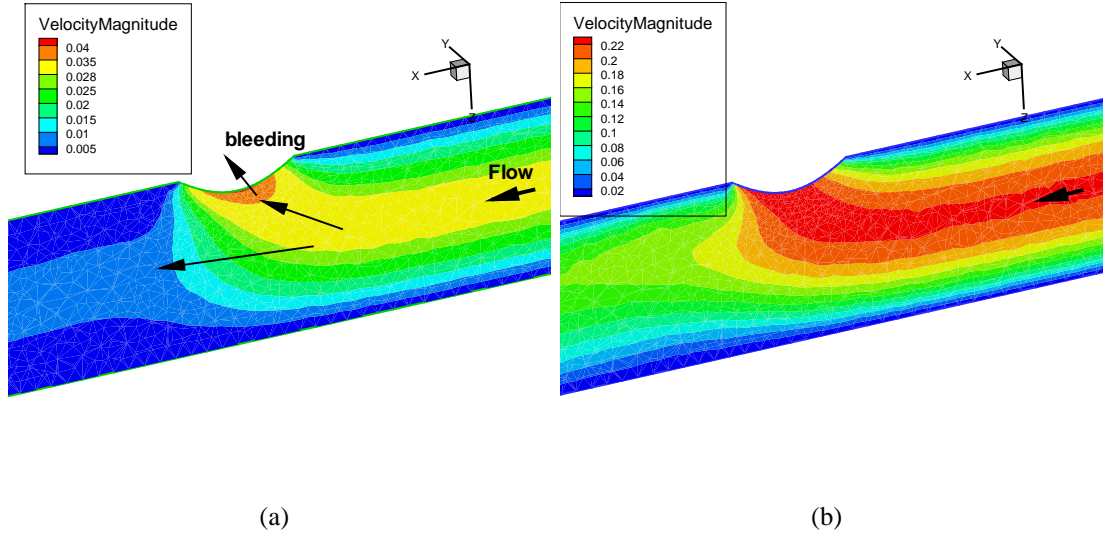


Fig. 3: The predicted velocity in vein (a) and artery (b) without acoustic streaming effect.

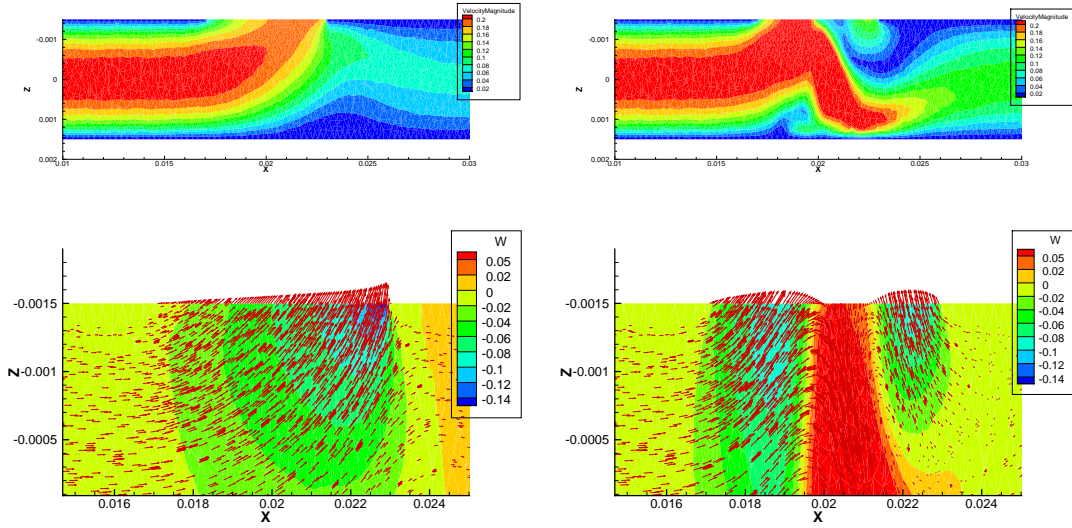


Fig. 4: The predicted velocity magnitude contours in the artery with the big wound for the cases with and without considering acoustic streaming. w - velocity in z direction.

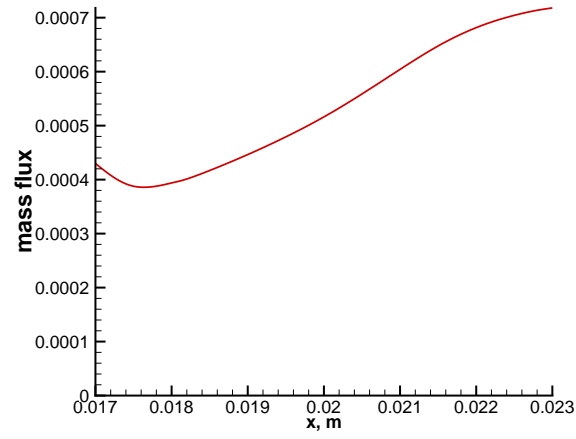


Fig. 5: The predicted mass flow at the big wound for the cases with different focal point locations, artery case.

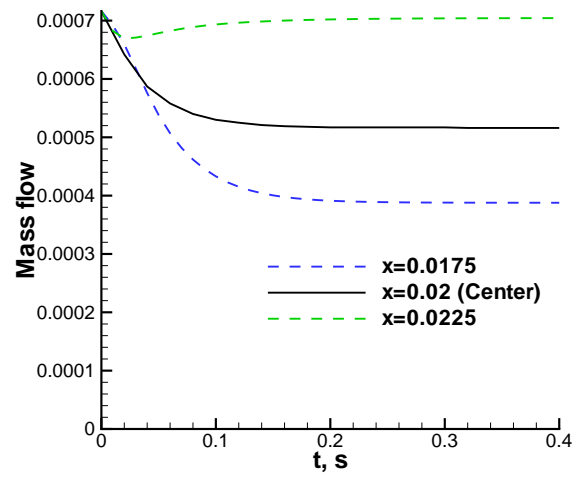


Fig. 6: The predicted mass flow with respect to time in the wound for the cases with different focal point locations, artery case.

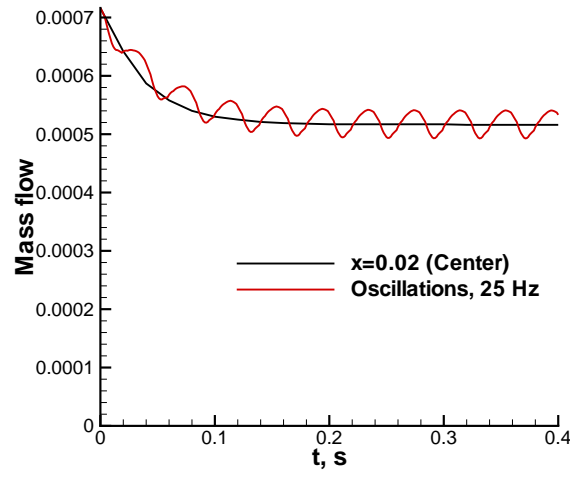


Fig. 7: The predicted mass flow with respect to time in the wound for two cases: 1) focal point is located at the center of the wound ($x = 0.02$); 2) focal point is oscillating around the center of the wound with the frequency 25 Hz .

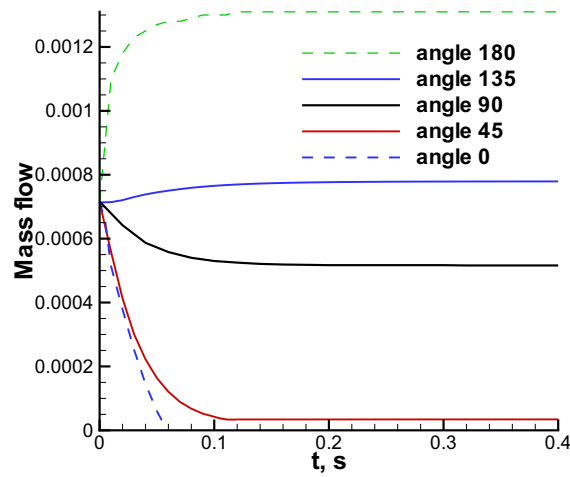


Fig. 8: The predicted mass fluxes with respect to time in the big wound for the cases with different sonication angles in the artery.

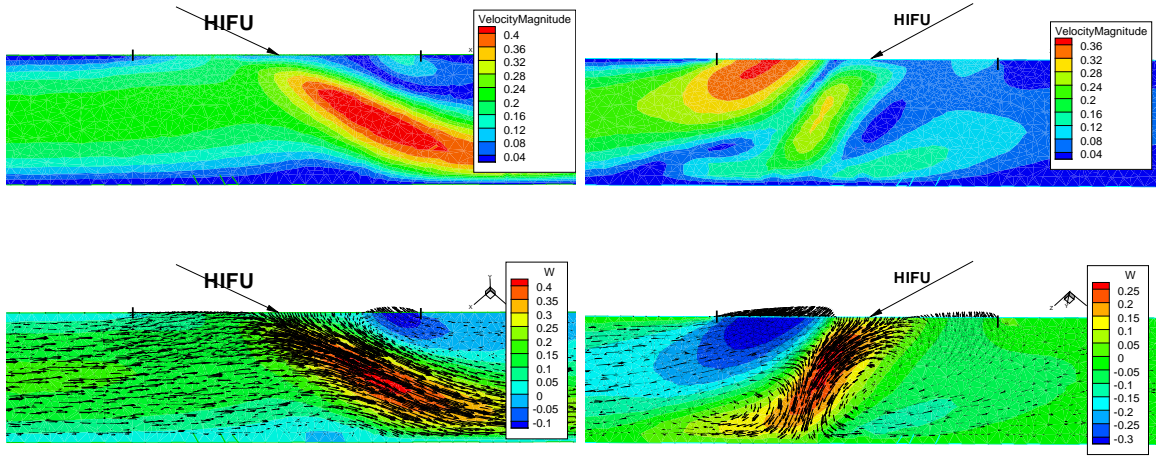


Fig. 9: The predicted velocity magnitude contours in the artery with the big wound for the sonication angles 45° and 135° . Focal point is located at the center of the wound in the artery. w - velocity in z direction.

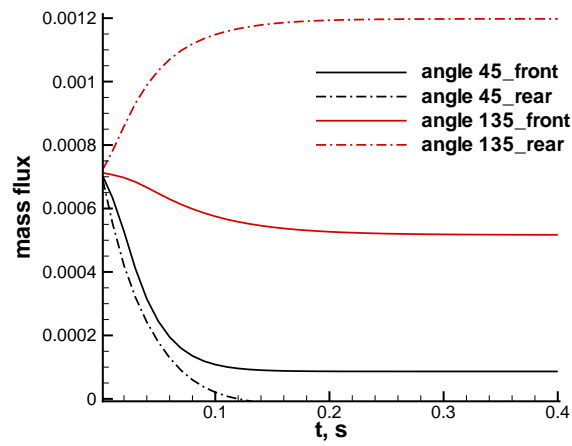


Fig. 10: The predicted mass fluxes with respect to time in the big wound for the cases with different sonication angles and different locations of the focal point in the artery.

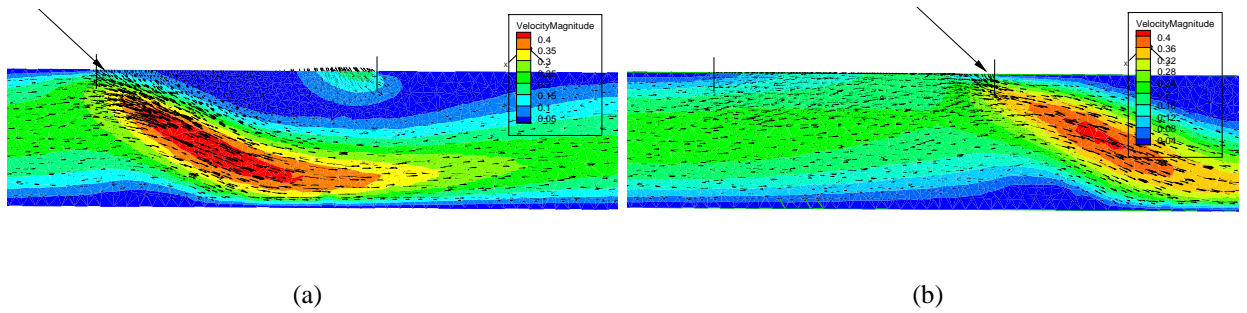


Fig. 11: The predicted velocity magnitude in the artery with the big wound for the cases with different locations of the focal point: (a) in front of the wound and (b) at the rear of the wound. The sonication angle is 45° .

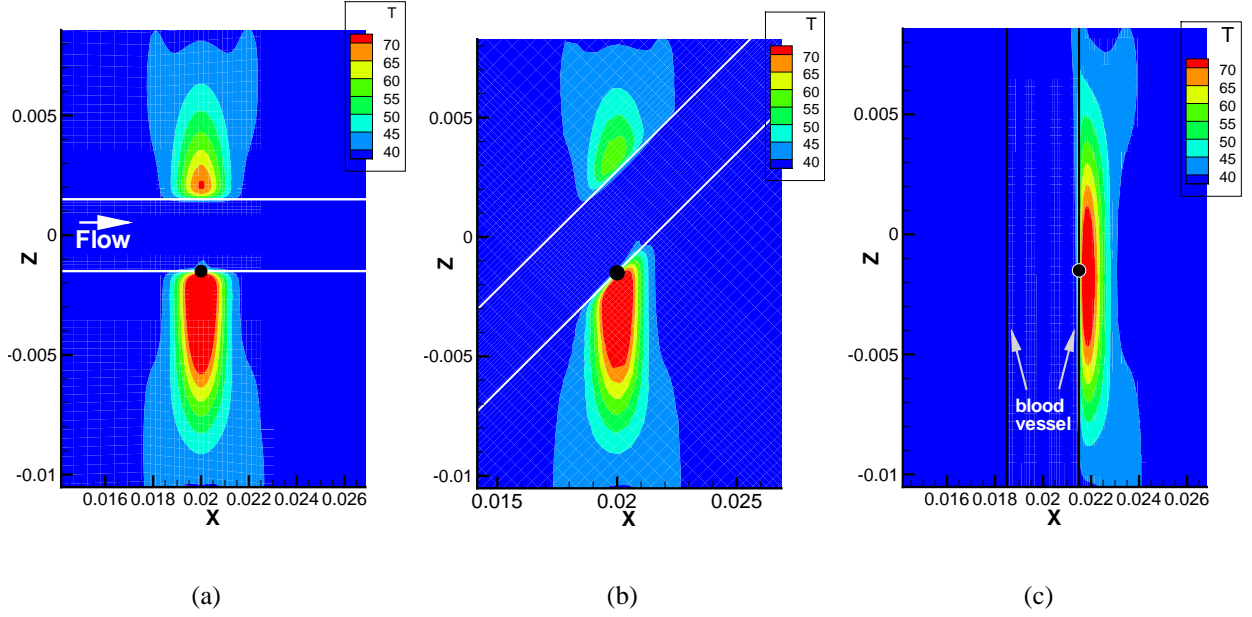


Fig. 12: The predicted temperature contours at $t = 0.6$ s at the cutting plane $y = 0$ for different sonication angles 90° (a), 45° (b) and 0° (c). Focal point (●) is located on the blood vessel wall.

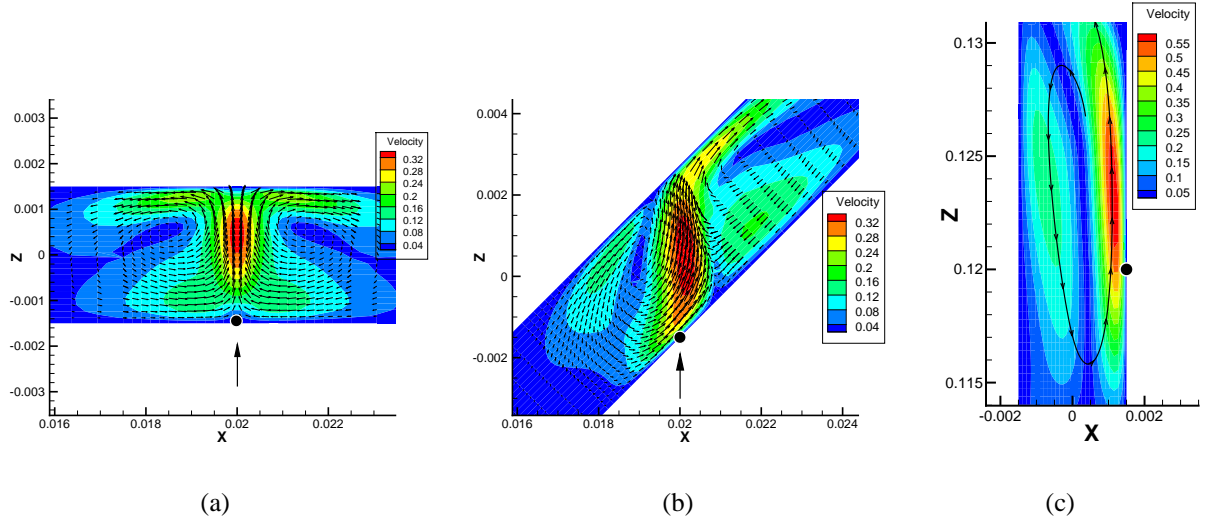


Fig. 13: The predicted acoustic streaming velocity vectors and magnitudes contours at the cutting plane in the blood vessel without an externally applied flow (blood flow=0) for different sonication angles 90° (a), 45° (b) and 0° (c). Focal point (●) is located on the blood vessel wall.

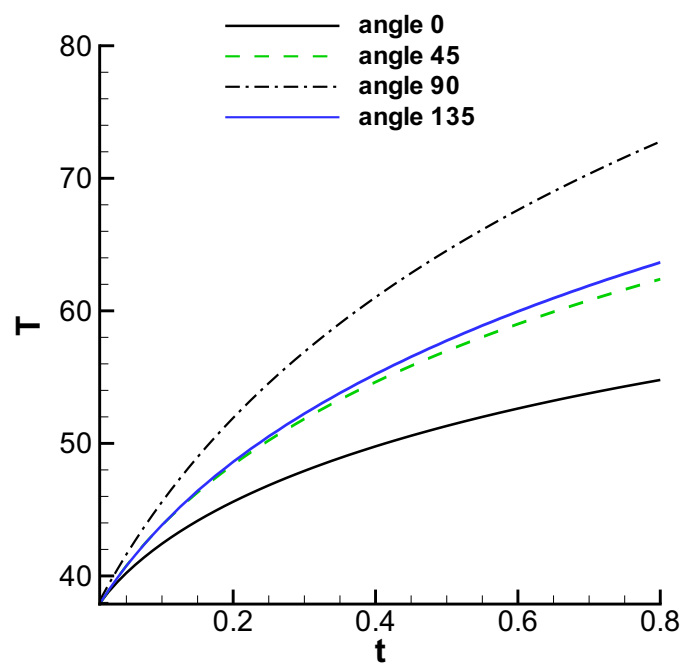


Fig. 14: The predicted temperature at the focal point as the function of time for different sonication angles.